

DFT Study of Internal Alkyne-to-Disubstituted Vinylidene Isomerization in $[\text{CpRu}(\text{PhC}\equiv\text{CAr})(\text{dppe})]^+$

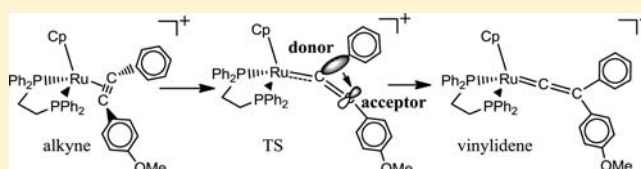
Miho Otsuka,[†] Noriko Tsuchida,^{*,†} Yousuke Ikeda,[‡] Yusuke Kimura,[‡] Yuichiro Mutoh,^{‡,§} Youichi Ishii,[‡] and Keiko Takano^{*,†}

[†]Department of Chemistry and Biochemistry, Graduate School of Humanities and Sciences, Ochanomizu University, Otsuka, Bunkyo-ku, Tokyo 112-8610, Japan

[‡]Department of Applied Chemistry, Faculty of Science and Engineering, Chuo University, 1-13-27 Kasuga, Bunkyo-ku, Tokyo 112-8551, Japan

S Supporting Information

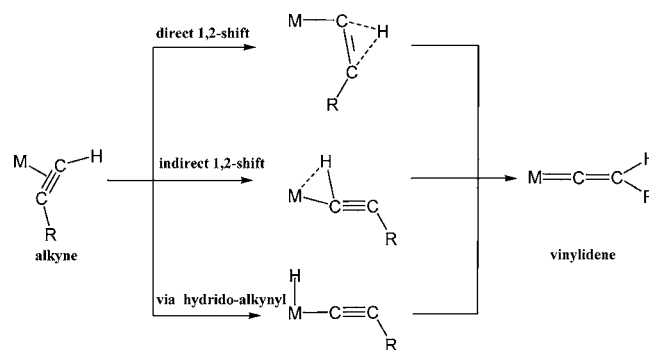
ABSTRACT: Internal alkyne-to-vinylidene isomerization in the Ru complexes ($[\text{CpRu}(\eta^2\text{-PhC}\equiv\text{CC}_6\text{H}_4\text{R-}p)(\text{dppe})]^+$ ($\text{Cp} = \eta^5\text{-C}_5\text{H}_5$; $\text{dppe} = \text{Ph}_2\text{PCH}_2\text{CH}_2\text{PPh}_2$; $\text{R} = \text{OMe}, \text{Cl}, \text{CO}_2\text{Et}$)) has been investigated using a combination of quantum mechanics and molecular mechanics methods (QM/MM), such as ONIOM(B3PW91:UFF), and density functional theory (DFT) calculations. Three kinds of model systems (I–III), each having a different QM region for the ONIOM method, revealed that considering both the quantum effect of the substituent of the aryl group in the η^2 -alkyne ligand and that of the phenyl groups in the dppe ligand is essential for a correct understanding of this reaction. Several plausible mechanisms have been analyzed by using DFT calculations with the B3PW91 functional. It was found that the isomerization of three complexes ($\text{R} = \text{OMe}, \text{CO}_2\text{Et}, \text{and Cl}$) proceeds via a direct 1,2-shift in all cases. The most favorable process in energy was path 3, which involves the orientation change of the alkyne ligand in the transition state. The activation energies were calculated to be 13.7, 15.0, and 16.4 kcal/mol, respectively, for the three complexes. Donor–acceptor analysis demonstrated that the aryl 1,2-shift is a nucleophilic reaction. Furthermore, our calculation results indicated that an electron-donating substituent on the aryl group stabilizes the positive charge on the accepting carbon rather than that on the migrating aryl group itself at the transition state. Therefore, unlike the general nucleophilic reaction, the less-electron-donating aryl group has an advantage in the migration.



1. INTRODUCTION

The acetylene-to-vinylidene rearrangement in the coordination sphere of a transition metal is a thermodynamically favorable process in most cases. This type of transformation reaction has been experimentally observed in mononuclear complexes¹ or in bi- and trinuclear derivatives.² The vinylidene complexes play important roles as intermediates in the synthesis of various organic compounds from alkyne complexes. In fact, there are a lot of examples that include vinylidene complexes in reaction pathways.³ Therefore, it is essential to establish a method for synthesizing vinylidene complexes. Great effort has been devoted to both experimental and theoretical approaches to determine the mechanism underlying the transformation of terminal alkynes into the corresponding vinylidene complexes.⁴ Theoretical studies suggested that the pathways of terminal-alkyne/vinylidene rearrangement are divided into two groups on the basis of the type of central metal. The d^6 metal systems such as Ru(II) and Mn(I) complexes proceed via either a direct 1,2-hydrogen shift or an indirect 1,2-hydrogen shift involving an alkyne intermediate with agostic interaction.^{5,6} In contrast, the isomerization of the d^8 metal systems such as Co(I) and Rh(I) progresses via a 1,3-hydrogen shift with a hydride-alkynyl intermediate (Scheme 1).⁷ For transformation from hydride-alkynyl intermediate to vinylidene product in the 1,3-hydrogen

Scheme 1. Conversion Pathways of an Alkyne Ligand to Vinylidene Isomer



shift process, two different mechanisms, uni- and bimolecular pathway, have been proposed. Recently, double crossover experiment and DFT calculations have demonstrated that the possibility of significant involvement of a bimolecular process was low.⁸ For the three pathways in Scheme 1, most theoretical

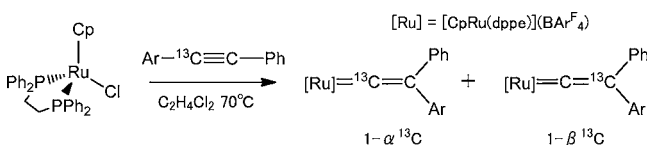
Received: August 12, 2012

Published: September 20, 2012

calculations concluded that the hydrogen migrations are electrophilic reactions.

The conversion reaction from internal alkynes to vinylidenes is an unusual process, and it has been reported only for heteroatom-substituted alkynes such as trimethylsilyl alkynes.⁹ Recently, the migration of acyl and hydrocarbyl substituents in internal alkynes has been reported by three groups independently.^{10–12} Shaw and co-workers described that internal alkyneones can participate in such interconversion to give disubstituted vinylidene complexes $[\text{CpRu}\{\text{C}=\text{C}=\text{CR}^1(\text{COR}^2)\}(\text{PPh}_3)_2]^+$.¹⁰ According to the reports by us, aryl- or alkyl-disubstituted vinylidene compounds have been obtained by the reaction of $[\text{CpRu}(\text{dppe})]^+$ and $[\text{CpFe}(\text{dppe})]^+$ with $\text{PhC}\equiv\text{CC}_6\text{H}_4\text{R}-p$ ($\text{R} = \text{OMe}, \text{Me}, \text{H}, \text{Cl},$ and CO_2Et), revealing the migratory activity of the substituents. The relative migratory aptitude increases in the order $\text{CO}_2\text{Et} > \text{Cl} > \text{H} > \text{Me} > \text{OMe}$ (See Scheme 2),^{11b} which suggests that

Scheme 2. Migratory Aptitude for Alkyne Substituents Reported in Ref 11a–c



Ar	Time	1- α - ^{13}C	:	1- β - ^{13}C	Isolated yield
$\text{C}_6\text{H}_4\text{OMe}-p$	1h	6	:	94	88
$\text{C}_6\text{H}_4\text{Me}-p$	1h	23	:	77	90
$\text{C}_6\text{H}_4\text{CO}_2\text{Et}-p$	12h	86	:	14	71
$\text{C}_6\text{H}_4\text{Cl}-p$	12h	55	:	45	89

aryl 1,2-migration proceeds as an electrophilic reaction. This is in accord with the previous theoretical calculations on the vinylidene rearrangement of the terminal alkynes,⁶ but is opposite to the generally accepted understanding of alkyl or aryl group migration, in which the migrating groups behave as nucleophiles. Valerga et al. also succeeded in synthesis of vinylidenes from internal alkyne complexes $[\text{TpRu}\{\eta^1\text{-O}=\text{C}(\text{R})\text{C}\equiv\text{CPh}\}(\kappa^2\text{P},\text{N}^i\text{Pr}_2\text{PXPY})]$ ($\text{X} = \text{CH}_2, \text{S}; \text{R} = \text{Me}, \text{Ph}$). DFT calculations were applied to their isomerization reactions. They concluded that the isomerization reactions of internal alkyne/vinylidene are electrophilic in the same manner as those of the terminal alkyne/vinylidene.^{12b} However, it was only based on the natural bond orbital (NBO) charges.

Meanwhile, Bassetti et al. stated their belief in the superiority of hydrogen migration as a hydride toward the electron-deficient C_α for terminal alkynes.¹³

In order to clarify the controversial issues whether or not the transformation of alkyne at a transition metal is an electrophilic reaction, quantum mechanics (QM) calculations were conducted for the rearrangement of internal alkynes to vinylidenes. In the present study, we report the computational results of DFT calculations on the transformation reaction of $[\text{CpRu}(\text{PhC}\equiv\text{CC}_6\text{H}_4\text{R}-p)(\text{dppe})]^+$ ($\text{R} = \text{OMe}, \text{CO}_2\text{Et},$ and Cl).

2. COMPUTATIONAL DETAILS

DFT calculations on $[\text{CpRu}(\text{PhC}\equiv\text{CC}_6\text{H}_4\text{R}-p)(\text{dppe})]^+$ ($\text{R} = \text{OMe}, \text{CO}_2\text{Et}$) were carried out to investigate the favorable isomerization pathways from internal alkyne complexes to the corresponding vinylidene complexes.

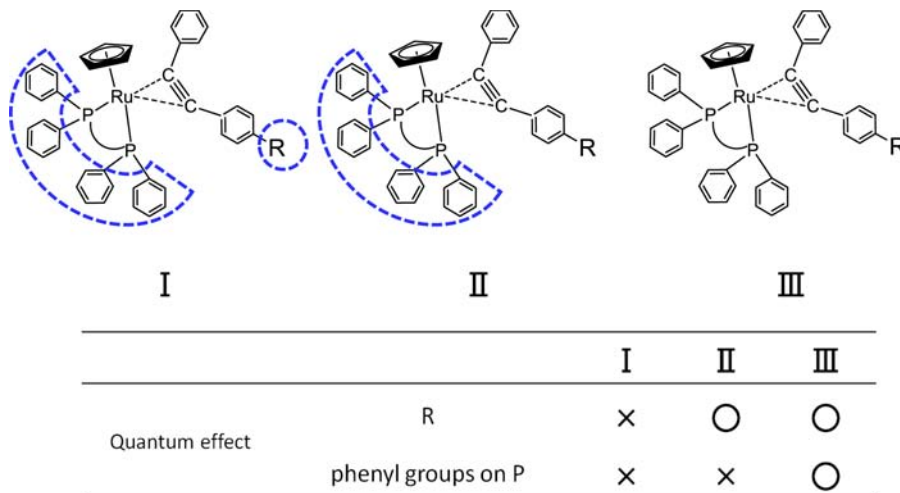
First, three kinds of model systems, denoted as models I–III, with different QM regions, were constructed to examine the quantum effect of the substituent in the aryl group and that of the phenyl groups linked to P atoms for the Ru complexes $[\text{CpRu}(\text{PhC}\equiv\text{CC}_6\text{H}_4\text{R}-p)(\text{dppe})]^+$ (see Scheme 3). In model system I, both a substituent on the aryl group ($\text{R} = \text{OMe}, \text{CO}_2\text{Et}$) and the phenyl groups linked to P atoms were treated as the molecular mechanics (MM) region. The MM region of model II includes phenyl groups linked to P atoms. Model III has no MM region; it consists only of QM regions.

The ONIOM calculations have been performed with a two-layer ONIOM(QM/MM) scheme, in which link atoms are treated as hydrogen atoms at the interface between the QM and MM regions.¹⁴ The total energy of the system is calculated by the following equation:

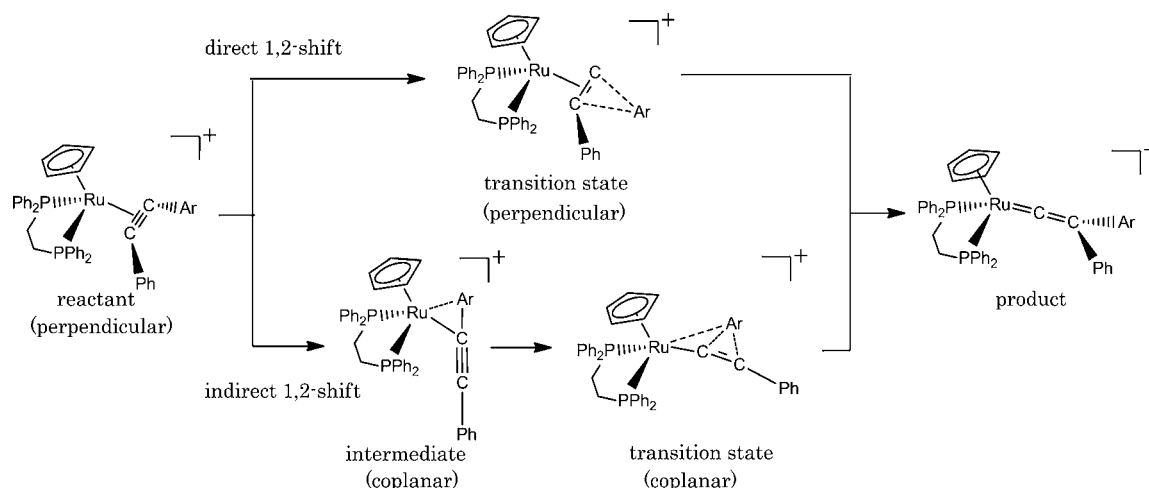
$$E_{\text{ONIOM}} = E_{\text{MM}(\text{real})} + E_{\text{QM}(\text{model})} - E_{\text{MM}(\text{model})}$$

$E_{\text{MM}(\text{real})}$ represents the MM energy of the entire system, i.e., the real system. $E_{\text{QM}(\text{model})}$ is the QM energy of the model system and is a chemically important part of it. $E_{\text{MM}(\text{model})}$ is the MM energy of the model system. Electrostatic interactions between the QM and MM layers were calculated by a mechanical embedding scheme. In the present ONIOM optimization calculations, a density functional theory

Scheme 3. Three Model Systems Used for ONIOM Calculations with Different QM/MM Regions^a



^aThe MM region is encircled by dotted lines.

Scheme 4. Proposed Reaction Mechanisms for Alkyne–Vinylidene Rearrangement on Ru Complex^{6–8,12b} in the Previous Studies^a

^aThe orientation of alkyne changes from perpendicular to coplanar with the Cp–Ru axis in the indirect 1,2-shift due to the interaction between the migrating group and Ru. In contrast, there is no interaction between them in the direct 1,2-shift.

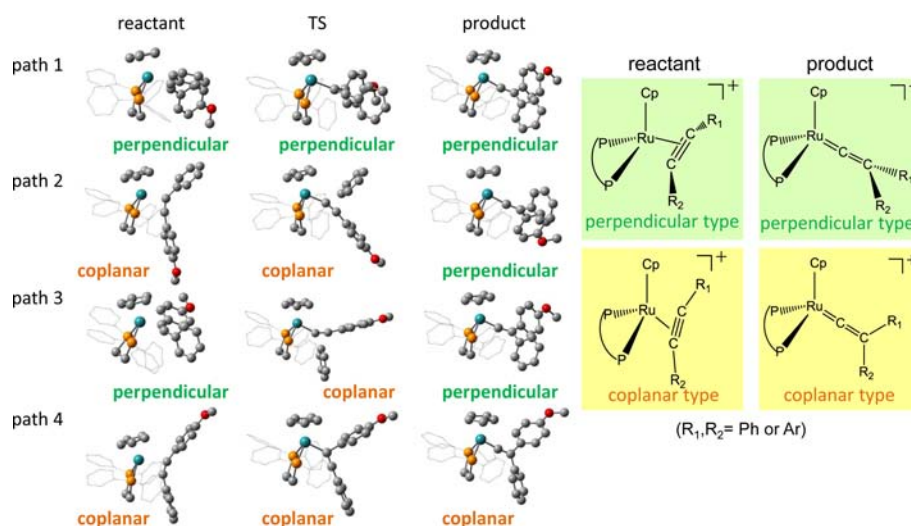


Figure 1. Optimized structures of the stationary points for $[\text{CpRu}(\text{PhC}\equiv\text{CC}_6\text{H}_4\text{OMe-}p)(\text{dppe})]^+$ in each reaction path at the B3PW91/LanL2DZ+6-31G(d) level. Hydrogen atoms are omitted for clarity. See Supporting Information for dihedral angles (Cp–Ru–C–R₂) of the reactant and product complexes for paths 1–4.

(DFT) with the hybrid functional B3PW91¹⁵ and MM calculation using the universal force field (UFF)¹⁶ were employed as a high-level QM method and a low-level MM method, respectively. For the DFT calculations, a LanL2DZ basis set with the effective core potential (ECP) of Hay and Wadt was used for the ruthenium atom.¹⁷ The 6-31G(d) basis set¹⁸ was chosen for the remaining atoms (C, H, O, P). The combined basis set is denoted as LanL2DZ+6-31G(d) in the present study.

The B3PW91/LanL2DZ+6-31G(d) method was used for the reaction pathway search of the whole system. The obtained structures were refined at the B3PW91 level with the following basis set: the Stuttgart/Dresden (SDD) ECP and corresponding basis set¹⁹ for Ru and the 6-31G(d) basis set for the remaining nonmetal atoms. The combined basis set is denoted here by SDD+6-31G(d). The geometry of the stationary points on the potential energy surface of $[\text{CpRu}(\text{PhC}\equiv\text{CC}_6\text{H}_4\text{R-}p)(\text{dppe})]^+$ (R = Cl) complex was also optimized for comparison at this level. All the stationary points were characterized by vibrational analysis as local minima (LM), transition states (TS), or higher-order saddle points.

All the calculations in the present study were performed using the Gaussian 09 program.²⁰ Linux PC cluster machines at Ochanomizu University and the computer facilities at the Research Center for Computational Science in Okazaki, Japan, were used.

3. RESULTS AND DISCUSSION

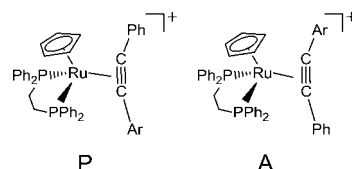
Energy Profiles and Geometries for Four Reaction Paths. In the alkyne–vinylidene rearrangement reaction at the Ru complex, two types of reaction pathway, the direct 1,2-shift and the indirect 1,2-shift, have been proposed on the basis of previous mechanistic studies on terminal alkynes and internal alkynes shown in Scheme 1.^{6–8,12b} If these processes are applied to the Ru complex in the present study, migration occurs with no interaction with the central metal for the direct 1,2-shift, whereas an intermediate in the indirect 1,2-shift pathway has a moving group that interacts with the central metal. In the latter case, the alkyne orientation changes from

perpendicular to coplanar with the Cp–Ru axis, as shown in Scheme 4.

According to the proposed mechanisms shown in Scheme 4, the reaction pathways for the Ru complexes (R = OMe, CO₂Et) were investigated by using the QM/MM [ONIOM-(B3PW91:UFF)] and DFT (B3PW91) methods. As a result, reaction paths 1–4 were obtained (see Figure 1). Path 1 proceeds via the direct 1,2-aryl shift without orientation change of the alkyne ligand between the reactant and the TS. An alkyne ligand of the reactant and the TS are located perpendicular to the Cp–Ru axis. The routes of paths 2–4 are similar to those of the indirect 1,2-shift. The alkyne group in the TS structure is located coplanar to the Cp–Ru axis in all cases. However, the bonding mode of the direct 1,2-shift is slightly different from that of the indirect 1,2-shift, because there is no bonding interaction between the leaving group and the central metal. Therefore, the transfer of the aryl group in paths 2–4 is the direct 1,2-shift, the same as in path 1. As mentioned above, the TS structures of paths 2–4 are quite similar, but the structures of the reactants or products derived from TS structures by intrinsic reaction coordinate (IRC) calculation²¹ are not the same. Several alkynes and vinylidenes are perpendicular to the Cp–Ru bond, and the others are coplanar, as shown in Figure 1. In the present paper, these orientations are denoted as perpendicular and coplanar types, respectively. The structure of path 1 changes as follows: perpendicular type (reactant) → perpendicular type (TS) → perpendicular type (product). The structural change of path 2 is “coplanar” → “coplanar” → “perpendicular”, that of path 3 is “perpendicular” → “coplanar” → “perpendicular”, and that of path 4 is “coplanar” → “coplanar” → “coplanar”. Table 1 lists the energy barriers in Gibbs free energy ($\Delta G_R = G_{TS} - G_{reactant}$, $\Delta G_P = G_{TS} - G_{product}$) for each path in models I–III. The Ru complexes have structural isomers that depend on the positions of the aryl and phenyl groups against the cyclopentadienyl (Cp) ring. The letters “P” and “A” represent phenyl group structures that take

the same and opposite positions to the Cp side, respectively (See Scheme 5). The numbers 1–4 in front of the letters P and A

Scheme 5. Two Geometric Isomers for the Ru Complex, Denoted as P and A, Which Correspond to the Positions of Ph and Ar Groups with Respect to the Cp Group



A show the path number from path 1 to path 4. For model I, three kinds of paths (paths 1, 2, and 4) were obtained (see Table 1). Whereas the aryl (Ar) migration of path 4A has the smallest ΔG_R (6.1 kcal/mol) in the case of R = OMe, the phenyl (Ph) migration on path 2P has the smallest one (4.3 kcal/mol) for R = CO₂Et. These results are the reverse of the experimental results (OMe, Ph migration 94%; CO₂Et, Ar migration 86%). Model II also has paths 1, 2, and 4 as reaction routes. For R = OMe, the lowest ΔG_R of Ar migration is 10.4 kcal/mol for path 4A and that of Ph migration is 9.6 kcal/mol for path 2P. Thus, there is only a small difference in ΔG_R between Ar and Ph migration. Similarly, there is a slight difference between the lowest ΔG_R of Ar migration and that of Ph migration for R = CO₂Et. The most plausible pathway for Ar migration of R = CO₂Et is path 2A ($\Delta G_R = 10.3$ kcal/mol), and that for Ph migration is path 4P (10.1 kcal/mol). Therefore, the results of model II also disagree with the experimental ones. These results from models I and II indicate that the quantum effect of the substituent in the aryl group (R) and that of the phenyl groups linked to P atoms are essential for the reaction.

The calculations based on model III, i.e., quantum chemical calculations for the whole system, gave paths 1–3. Ph migration on path 2P has the smallest activation energy (8.0 kcal/mol) in R = OMe, while that of R = CO₂Et was Ar migration on path 2A (10.8 kcal/mol). As mentioned above, the structures of the reactant are different among the paths, i.e., the reactants have different relative stabilities. A comparison of the energy of each reactant shows that the one in path 2 (in the coplanar type) is less stable than those in paths 1 and 3 (perpendicular type) by 4.7 kcal/mol. Consequently, the reaction barrier of path 2 is lower than those of paths 1 and 3. The energy profiles of the transformation from the perpendicular type to the coplanar type for R = OMe and CO₂Et are shown in Figure 2. For R = OMe (solid line), the minimum and maximum energies are, respectively, –6.5 and +2.0 kcal/mol. The energy difference between them, which corresponds to the rotation barrier, is 8.5 kcal/mol, whereas that of R = CO₂Et (dashed line) is approximately 11 kcal/mol. These values are lower than the activation energies of the rate-determining steps (Ar or Ph migration) of both paths 1 and 3. Therefore, path 2 is the most plausible reaction path at this calculation level. All paths proceed through the direct 1,2-shift of the carbon substituent and have only one transition state (TS), as was the case in the previous studies by Valerga et al.^{12b} Whereas the isomerization of the terminal alkyne Ru complexes proceeds via direct 1,2-shift or indirect 1,2-shift, the internal alkyne complexes are allowed only the direct 1,2-shift. It is because the migrating Ar (or Ph) groups with a hybridized sp² orbital configuration have

Table 1. Energy Barriers (kcal/mol) in Gibbs Free Energy ($\Delta G_R = G_{TS} - G_{reactant}$, $\Delta G_P = G_{TS} - G_{product}$) for Each Path in Models I–III at the B3PW91/LanL2DZ+6-31G(d) Level

R	model	Ar migration (OMe, 6%; CO ₂ Et, 86%)			Ph migration (OMe, 94%; CO ₂ Et, 14%)		
		path	ΔG_R	ΔG_P	path	ΔG_R	ΔG_P
OMe	I	1	9.3	24.0	1	13.9	24.3
		2P	11.8	21.9	2P	8.8	23.7
		4A	6.1	17.3	2A	13.3	23.5
	II	1	18.5	31.7	1	16.9	29.3
		2P	14.7	24.1	2P	9.6	18.4
		4A	10.4	16.0	2A	13.6	20.1
	III	1	20.4	26.0	1	N/A	
		2P	13.8	24.6	2P	8.0	18.1
		3A	15.0	22.2	3A	15.8	21.8
CO ₂ Et	I	1	15.9	30.1	1	14.7	28.8
		2P	17.8	26.8	2P	4.3	22.9
		2A	N/A		2A	14.9	26.2
	II	1	13.0	27.7	1	15.2	27.3
		2P	14.3	22.6	4P	10.1	17.1
		2A	10.3	22.3	2A	13.2	27.7
	III	1	20.4	27.4	1	N/A	
		3P	18.8	25.4	3P	17.1	24.1
		2A	10.8	22.9	3A	18.9	26.9

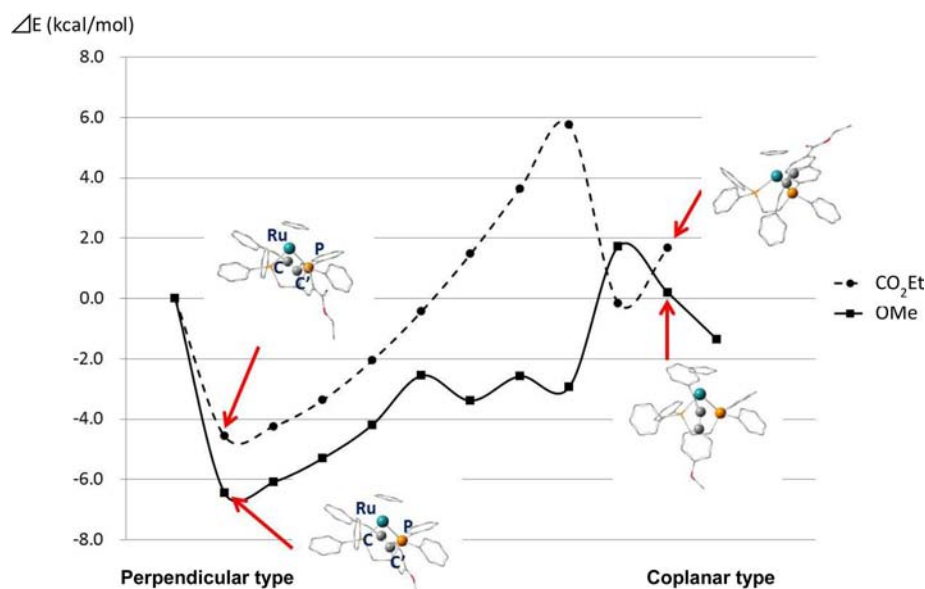


Figure 2. Energy profiles and geometries for scan calculations from the perpendicular type to the coplanar type resulted at B3PW91/LanL2DZ+6-31G(d) (kcal/mol). To clarify the conformation change, the atoms that are related to the rotational angle are shown as balls and sticks. Solid and dashed lines are, respectively, for R = OMe and CO₂Et.

a limited orientation in binding with the carbon of the C≡C. In contrast, it is easier to have a three-center interaction of Ru–carbon(Ar)–carbon(C≡C) due to the s orbital character in the H atom.

Refinement of the Reaction Paths by Using SDD ECPs.

Starting from the reaction path obtained on the basis of model III at the B3PW91/LanL2DZ+6-31G(d) level, refining calculations at the B3PW91/SDD+6-31G(d) level were carried out. Table 2 lists the activation energies for Ar and Ph

Table 2. Energy Barriers (kcal/mol) in Gibbs Free Energy ($\Delta G_R = G_{TS} - G_{reactant}$, $\Delta G_P = G_{TS} - G_{product}$) for Each Path in Model III at the B3PW91/SDD+6-31G(d) Level

R	model	Ar migration			Ph migration		
		path	ΔG_R	ΔG_P	path	ΔG_R	ΔG_P
OMe	III	1	21.3	29.3	1	N/A	
		3P	18.0	26.7	3P	13.7	21.1
		3A	15.7	25.2	3A	15.5	23.2
CO ₂ Et	III	1	21.6	30.4	1	23.7	30.9
		3P	18.7	27.3	3P	17.2	26.5
		3A	15.0	24.5	3A	19.1	28.7
Cl	III	1	22.0	29.6	1	23.4	31.5
		3P	17.6	26.5	3P	16.5	25.4
		3A	16.4	24.6	3A	18.9	26.7

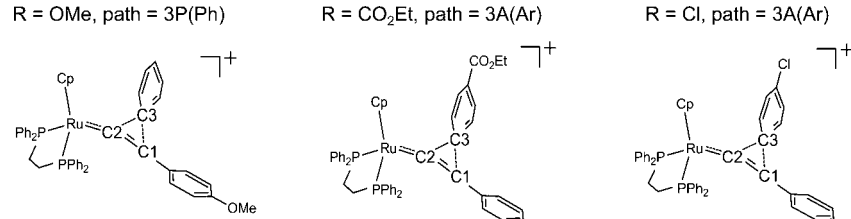
migration. Only paths 1 and 3 were obtained. Comparing ΔG_R of path 1 with that of path 3, we find that path 3 has lower ΔG_R than path 1 for any substituents (R). The path giving the smallest ΔG_R in each R is the Ph migration for R = OMe (13.7 kcal/mol) and the Ar migration for R = CO₂Et (15.0 kcal/mol). These findings agree with the experimental results that Ph tends to migrate more easily for R = OMe, but with more difficulty for R = CO₂Et. Additionally, the result that ΔG_R of R = OMe is lower than that of R = CO₂Et also agrees well with the experimental finding that the reaction rate of R = OMe is faster than that of CO₂Et (OMe, 1 h; CO₂Et, 12 h). To assess the appropriateness of the resulting pathway, additional

calculations for R = Cl were performed. These results also showed that path 3 has the lowest energy barrier (see Table 2). The ΔG_R of path 3 is almost the same between Ar migration (16.4 kcal/mol) and Ph migration (16.5 kcal/mol), which is in good agreement with the experimentally reported migration aptitude (Ar:Ph = 55%:45%). These results reveal that the isomerization reaction of internal alkynes to vinylidenes proceeds through path 3.

As mentioned in the preceding section, a reactant complex has two types of structures, depending on the position of the aromatic rings of the internal alkynes. Therefore, there are two types of pathways in path 3, denoted as 3P and 3A, after the notation of the structures of the reactant P and A, respectively. The ΔG_R of 3P for R = OMe indicates that Ph migration has an advantage over Ar migration by 4.3 (=18.0 – 13.7) kcal/mol, while the energy of Ph migration for 3A is 15.5 kcal/mol and comparable to that of Ar migration, 15.7 kcal/mol. In contrast, there is no difference in migration energies between Ph and Ar groups for 3P of R = CO₂Et, but Ar migration has an advantage over Ph migration in 3A by 4.1 (=19.1 – 15.0) kcal/mol. For R = Cl, the migration energies are comparable between 3A and 3P. For R = OMe and CO₂Et, the $\Delta\Delta G_R$ between Ar and Ph migration differs depending on the structure of the reactant, 3P or 3A. Therefore, whether the structure of the reactant is P or A could be a causative factor in the preference of the reaction path.

TS Structures and Energy Profiles along the IRC Path.

To investigate paths 3A and 3P in detail, we compared the TS structures and energy profiles derived from the IRC calculations. Table 3 lists C1–C2–C3 angles and imaginary frequencies, where “C3” corresponds to a migrating carbon atom. Comparing the angle α (C1–C2–C3) in each R, the α values of Ar migration for R = OMe are 96°–98° and those of Ph migration are 73°–74°. Namely, in the case of R = OMe, the angle α in the TS is smaller for the preferable Ph migration than for Ar migration in both paths 3A and 3P. In contrast, the TS for Ar migration has a smaller α in the case of R = CO₂Et. The angles α of TS are comparable in their migration reactions

Table 3. Angles $\alpha(\text{C1}-\text{C2}-\text{C3})$ in deg for TS Structures and Imaginary Frequencies in cm^{-1} for Paths 3A, 3P, and 1 for Each Substituent (R = OMe, CO_2Et , and Cl)^a


R	model	Ar migration			Ph migration		
		path	$\alpha(\text{C1}-\text{C2}-\text{C3})$	freq (cm^{-1})	path	$\alpha(\text{C1}-\text{C2}-\text{C3})$	freq (cm^{-1})
OMe	III	1	97.8	91i	1	N/A	
		3P	98.2	65i	3P	73.6	259i
		3A	96.1	78i	3A	73.0	248i
CO_2Et	III	1	85.0	71i	1	95.5	55i
		3P	81.5	116i	3P	89.2	81i
		3A	80.8	140i	3A	91.9	55i
Cl	III	1	92.2	39i	1	90.6	43i
		3P	85.1	79i	3P	85.3	91i
		3A	85.2	89i	3A	85.8	71i

^aC3 is a carbon of the migrating group. Hydrogen atoms are omitted for clarity.

between Ar and Ph for R = Cl. The difference in α for the migration reactions between Ar and Ph with the same R is closely related to that of the experimental migration aptitude.

Figure 3 shows the energy profiles obtained from IRC calculations. Path 3A for R = OMe has almost the same reaction barriers, ΔG_{R} , for the Ar and Ph migrations. Compared to the Ar migration, Ph migration has a more glacial slope of energies from the reactant to the TS (see Figure 3a). This means Ph may migrate more easily than Ar on path 3A for R = OMe, even though they need equal amounts of free energies, ΔG_{R} , for migration. The tendency is the reverse for R = CO_2Et . As for the case of R = Cl, the energy profiles for the two paths coincide with each other, and there is a very small difference between the Ar and Ph migrations for both paths 3A and 3P. These results mean that a favorable rearrangement reaction is the Ph migration for R = OMe and the Ar migration for R = CO_2Et , even if the initial structure is A or P.

NBO Charges of Reactant Complexes. Table 4 lists NBO charges of the reactant on the most probable path in the case of each substituent R, where “C3” is the carbon atom that is going to migrate in this reaction, as discussed in the preceding section. The difference in substituents (R) has no influence on the NBO charges of the central Ru atom. These charges are negative in all cases and increase as the reaction proceeds. This could be due to the electron donation from ligands. In contrast, the substituents significantly influence the charges of carbon atoms located in the reaction center. For all cases, C1 and C2 have positive charges in the reactant complexes. Whereas there is a small difference in charges between C1 and C2 for R = OMe and CO_2Et , the value of C2 is twice larger than that of C1 for R = Cl. In the TS, the NBO charges of C2 are more positive than the reactant for R = OMe and become negative for R = CO_2Et and Cl. On the other hand, those of C1, which accepts the migration group, tend to greatly increase in the positive direction from the reactant to the TS and change into a negative charge at the product for all cases. C3 and C4 for all cases have negative charges through the reaction. In the reactants, the NBO charges on C3 and C4 are, respectively, -0.098 and -0.141 for R = OMe, and -0.062 and

-0.090 for R = CO_2Et . C3 in both cases is less negatively charged than C4, while the charge of C3 for R = Cl was similar in magnitude to that of C4. In all cases the values of migration carbon C3 decrease slightly in the TS and the product, but remain negative. The charge variations on C1 and C2 described above agree well with the assertion by Bassetti et al.¹³ that the hydrogen migrates as hydride toward the electron-deficient carbon in vinylidene/terminal-alkyne isomerization reaction based on both the kinetic study by itself and the previously reported theoretical works.

Table 5 lists the NBO charges in the migrating aromatic groups, i.e., phenyl group ($\text{R}_1 = \text{H}$) for R = OMe and aryl group for R = CO_2Et and Cl. The charge of each carbon includes that of hydrogen for C1, C2, C4, and C5 and substituents R_1 ($\text{R}_1 = \text{H}$ for R = OMe, $\text{R}_1 = \text{CO}_2\text{Et}$ for R = CO_2Et , and $\text{R}_1 = \text{Cl}$ for R = Cl). Sum(1–5) for C3 is the summation of the group charges for C1–C5 including H and R_1 . The sum(1–5) values for all the cases are positive and reach the maximum values at the TS, which are $+0.293$ for R = OMe, $+0.189$ for R = CO_2Et , and $+0.186$ for R = Cl, respectively. These charge distributions are quite similar to those in common aromatic or alkyl nucleophilic migration.

The results mentioned in this section suggest that the alkyne/vinylidene transformation is caused by nucleophilic migration of the aryl group.

Donor–Acceptor Interaction. The NBO analysis has already proven to be an effective tool for the chemical interpretation of hyperconjugative interaction and electron density transfer. To investigate the various second-order interactions between the occupied and vacant orbitals, the HF/SDD+6-31G(d) level has been used, and it predicts the delocalization or conjugation. The interaction energy was deduced from the second-order perturbation approach:

$$E = \Delta E_{ij} = q_i \frac{F(i, j)^2}{(\epsilon_j - \epsilon_i)}$$

where $F(i, j)^2$ is the Fock matrix element between the i and j NBO orbitals, ϵ_i and ϵ_j are the NBO orbital energies, and q_i is

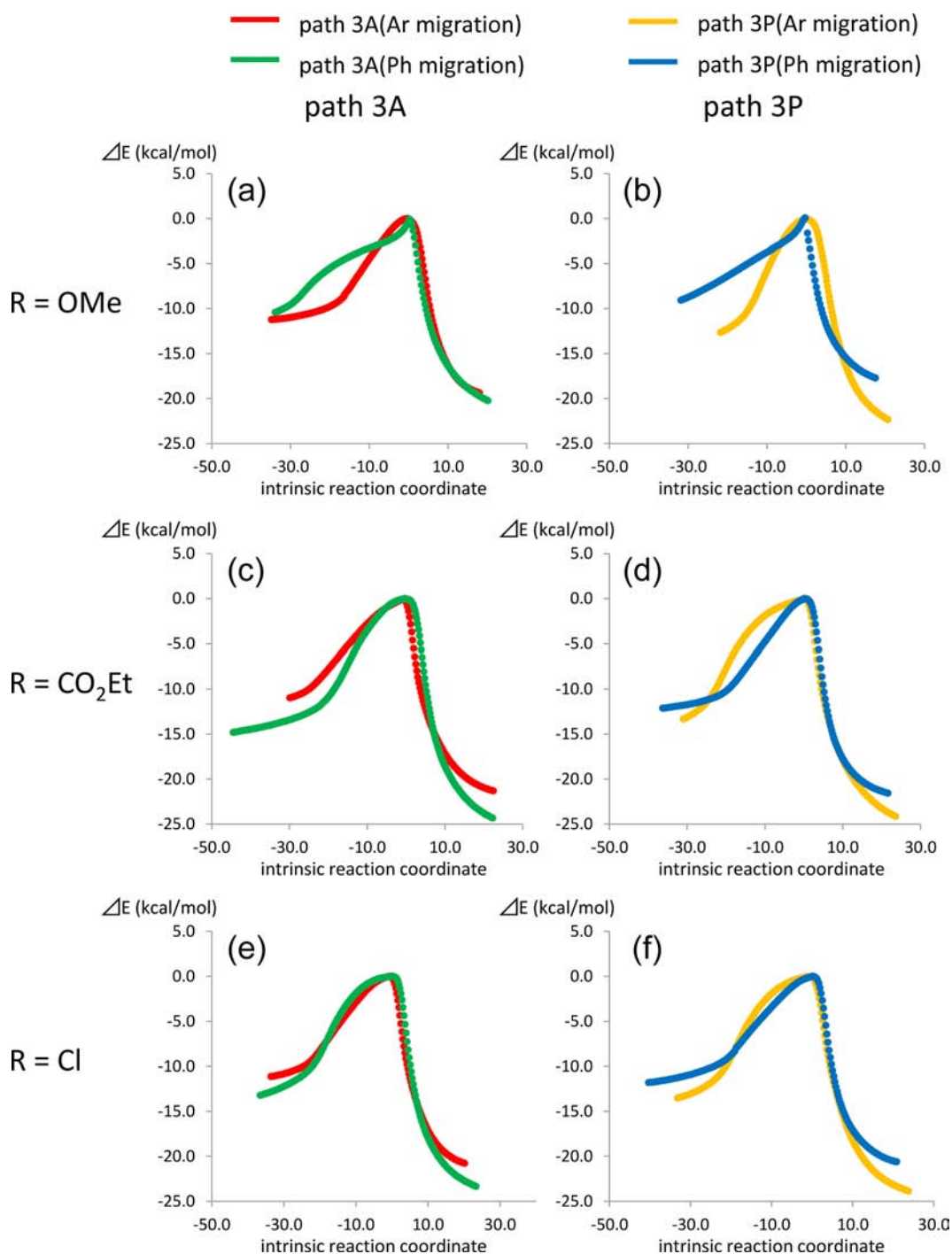


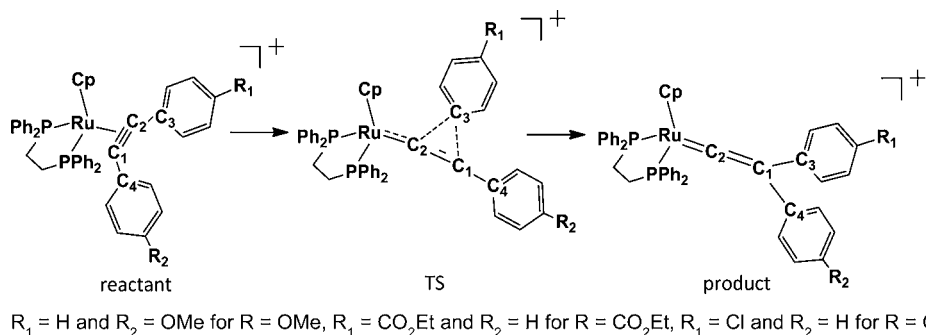
Figure 3. Energy profiles of path 3 that resulted from IRC calculations for each substituent ($R = \text{OMe}$, CO_2Et , and Cl) at the B3PW91/SDD+6-31G(d) level [red, path 3A (Ar migration); yellow, path 3P (Ar migration); green, path 3A (Ph migration); blue, path 3P (Ph migration)].

the population of the donor orbital.²² To examine whether the migration is electrophilic or nucleophilic, the interaction energies between the bonding π orbitals—BD(C2–C3) and BD(C4–C6)—and the vacant lone-pair orbitals—LP*(C1)—have been calculated using NBO analysis. Table 6 lists the interaction energies between the donor and acceptor for the cases with the smallest energy barriers of path 3P for $R = \text{OMe}$, 3A for $R = \text{CO}_2\text{Et}$, and 3A for $R = \text{Cl}$ (see Table 2). For entry 1, there is strong interaction between C2–C3 as an electron donor and C1 as an electron acceptor. The electron is transferred from a carbon on the migrating group to the one

being migrated. Other entries, such as 7, 9, and 11, also show the same type of interaction, although the energy values are different from each other. Thus, the migration reaction in the studied complexes is found to be nucleophilic.

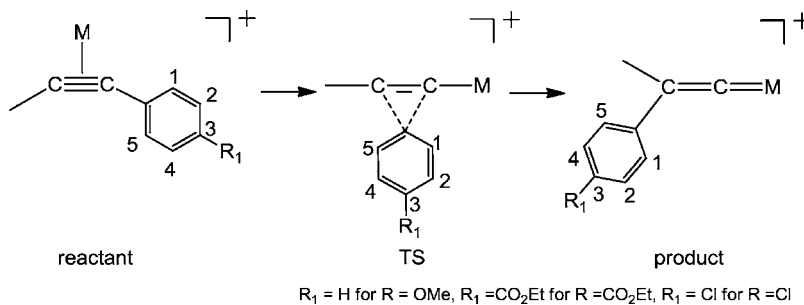
The theoretical findings mentioned above contradict the experimental results that the electron-withdrawing groups enhance the migratory aptitude. The product ratios of the reaction suggest that the migration reaction is electrophilic. Therefore, in our previous papers, we suggested that the alkyne/vinylidene rearrangement was more likely to occur via electrophilic reaction from the results of migratory aptitude.¹¹

Table 4. NBO Charge of the Most Probable Pathways for Each Complexes



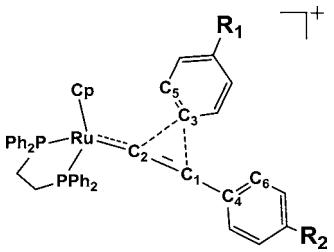
		reactant	TS	product
OMe	Ru	-0.776	-0.865	-0.918
	Cl	+0.025	+0.082	-0.205
	C2	+0.025	+0.036	+0.407
	C3	-0.098	-0.081	-0.057
	C4	-0.141	-0.217	-0.113
CO ₂ Et	Ru	-0.779	-0.865	-0.914
	Cl	+0.021	+0.172	-0.220
	C2	+0.025	-0.022	+0.415
	C3	-0.062	-0.032	-0.020
	C4	-0.090	-0.207	-0.064
Cl	Ru	-0.776	-0.861	-0.914
	Cl	+0.012	+0.212	-0.215
	C2	+0.030	-0.050	+0.410
	C3	-0.101	-0.053	-0.059
	C4	-0.090	-0.226	-0.065

Table 5. NBO Charges in the Migrating Groups through the Reaction



R	path		reactant	TS	product
OMe	3P(Ph)	1	+0.065	+0.106	+0.048
		2	+0.020	-0.004	+0.023
		3	+0.038	+0.093	+0.021
		4	+0.011	-0.003	+0.013
		5	+0.019	+0.101	+0.004
		sum(1-5)	+0.153	+0.293	+0.109
CO ₂ Et	3A(Ar)	1	+0.049	+0.060	+0.031
		2	+0.096	+0.079	+0.102
		3	-0.147	-0.103	-0.164
		4	+0.104	+0.097	+0.106
		5	+0.001	+0.056	-0.012
		sum(1-5)	+0.103	+0.189	+0.063
Cl	3A(Ar)	1	+0.086	+0.069	+0.068
		2	+0.026	+0.019	+0.030
		3	-0.019	+0.003	-0.035
		4	+0.016	+0.018	+0.018
		5	+0.039	+0.077	+0.025
		sum(1-5)	+0.148	+0.186	+0.106

Table 6. Conjugative Interaction Energies Based on the Second-Order Perturbation Theory Analysis of the Fock Matrix in the NBO Basis and Orbital Hybrids (s, p, d) of the Acceptor Orbital, LP*(C1), for TS Structures of the Three Ru Complexes



R	path (migration group)	R ₁	R ₂	entry	donor	acceptor	E(kcal/mol)	hybrids for LP*(C1) (%) (s, p, d)
OMe	3P (Ph)	H	OMe	1	C2–C3	Cl	231.95	(7.63, 92.22, 0.15)
				2	C4–C6	Cl	60.15	
	3P (Ar)	OMe	H	3	C2–C3	Cl	39.34	(0.26, 99.72, 0.02)
				4	C4	Cl	249.12	
CO ₂ Et	3A (Ph)	H	CO ₂ Et	5	C2–C3	Cl	63.92	(0.67, 99.28, 0.05)
				6	C4–C6	Cl	83.31	
	3A (Ar)	CO ₂ Et	H	7	C2–C3	Cl	144.32	(3.37, 96.52, 0.12)
				8	C4–C6	Cl	71.94	
Cl	3A (Ph)	H	Cl	9	C2–C3	Cl	94.85	(1.65, 98.27, 0.08)
				10	C4–C6	Cl	79.45	
	3A (Ar)	Cl	H	11	C2–C3	Cl	103.26	(1.96, 97.96, 0.08)
				12	C4–C6	Cl	81.65	

However, the reaction mechanism that the migrating groups move as a nucleophilic reagent is elucidated by the minute NBO analysis in the present study. Why, then, does the migratory reaction for R = OMe prefer, as a migrating group, the phenyl group with lower nucleophilic reactivity instead of the aryl group? A comparison of charge transfer energies of Ph migration and Ar migration for R = OMe illustrates the reason. For Ph migration, the energy of charge transfer from the donor (C2–C3) on the phenyl side to the acceptor C1 is 231.95 kcal/mol, much larger than the 60.15 kcal/mol interaction energy from the donor (C4–C6) in the aryl group to the C1 carbon. Thus, the strong interaction between the migrating phenyl group and the accepting carbon atom to be migrated causes the phenyl migration. In contrast, the stability derived from Ar migration (39.34 kcal/mol) is much lower than that from Ph migration (231.95 kcal/mol). Furthermore, the interaction between the Ph group (C4), which stays at the C1 site as a donor, and C1 as an acceptor is quite large (249.12 kcal/mol). This strong interaction between the Ph group and the acceptor (C1) prevents the Ar group from migrating to the C1 carbon. As for the complex with R = CO₂Et, entry 7 is dominant. The large value of 144.32 kcal/mol corresponds to the strong interaction between C2–C3 as an electron donor and C1 as an electron acceptor. There is only a small difference between Ph migration and Ar migration for the case of R = Cl, which is consistent with the experimental results. These results revealed that the charge transfer energies between an aromatic ring and a CC triple bond reflect the migratory aptitude.

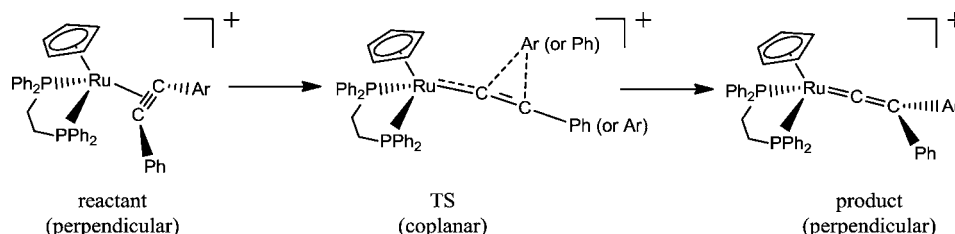
Generally, substituents on aryl group could affect the stabilization of the migration group in TS of the aryl transfer reaction. However, the migration aptitude in our alkyne/vinylidene rearrangement reaction is not consistent with this frame in the way that the less-electron-donating Ar group is easier to migrate than the other group in spite of the nucleophilic reaction. To understand the effect of the substituents on the TS, it is required to find out the influence on the acceptor carbon, which is one of the essential factors for

migration reaction. Orbital hybridization of the vacant lone pair orbitals [LP*(C1)] was analyzed. The s character in the orbital of acceptor carbon [LP*(C1)] at the Ph migration, 7.63%, is larger than that of the Ar migration for R = OMe, 0.26%, and the tendency for R = CO₂Et is the opposite. As for the Ph migration pathways, the s characters of LP*(C1) for R = Cl and CO₂Et, 1.65 and 0.67%, are much smaller than for R = OMe. The electron-donating substituent increases the s character on the acceptor carbon. The increase in the s character means that the acceptor carbon takes on a more widely binding orientation and facilitates a bond formation with the migrating group. Therefore, the Ph migration is preferable to Ar migration for R = OMe. The substituents of the Ar group affect the s orbital character of the acceptor carbon in the C≡C part.

It would be useful to comment on the qualitative interpretation of the calculation results in the present study. As already mentioned, in common organic nucleophilic rearrangement, it is widely accepted that an electron-donating substituent enhances the migratory aptitude of the aryl group by stabilizing a partial positive charge on the aryl group at the TS. In contrast, in the present case, the reaction path of the migration is controlled by the stabilization of a partial positive charge on the acceptor carbon (C1 in Table 6). Thus, although the vinylidene rearrangement of diaryl alkynes is nucleophilic in nature, the more-electron-rich aryl group is expected to stay on the C1 atom, and as a result, the other (the less electron-donating) aryl group migrates from the C2 atom. This effect accounts for the apparent discrepancy on the order of the migratory aptitude of aryl groups.

4. CONCLUSION

In the present study, the isomerization mechanism of internal alkyne complexes, [CpRu(PhC≡C₆H₄R-p)(dppe)]⁺ (R = OMe, CO₂Et), to the corresponding vinylidene complexes has been investigated to clarify the quantum effects from the substituents of the aryl group and from the phenyl groups of dppe ligands, how the aryl migration proceeds, and why the

Scheme 6. Plausible Reaction Pathway for $[\text{CpRu}(\text{PhC}\equiv\text{C}_6\text{H}_4\text{R}-p)(\text{dppe})]^+$ (R = OMe, Cl, and CO_2Et)

migratory aptitude increases with the electron-withdrawing properties of substituents in the aryl group. Three kinds of model systems (I–III), having different quantum mechanics regions, were constructed, and the density functional theory calculations [ONIOM(B3PW91:UFF) and B3PW91] were applied. Whereas the results of models I and II, which contain MM region, disagree with the experimental ones, that of model III, which corresponds to all QM calculations, agrees well with the experimental results. Thus, the quantum effects of the substituents on both the aryl group and the phosphine ligands are essential for this reaction.

On the basis of the calculated reaction paths for model III, which consists only of QM calculations, further calculations at the higher B3PW91/SDD+6-31G(d) level for three kinds of internal alkyne with the additional R = Cl system were carried out. Two types of 1,2-migration path were obtained, which differ from each other in their TS structures in paths 1 and 3. The activation free energy, ΔG_{R} , of path 3 is smaller than that of path 1 for any substituents (R). There are two types of pathway (3P and 3A) in path 3, where the structures of the reactant are different. The path having the smallest ΔG_{R} among 3P and 3A, respectively, is Ph migration via path 3P for R = OMe (13.7 kcal/mol) and Ar migration via path 3A for R = CO_2Et (15.0 kcal/mol), while the activation free energies are almost the same between Ar migration and Ph migration in both 3P and 3A for R = Cl. In addition, analysis of energy profiles along the IRC shows that the Ph migration has a more gradual slope from the reactant to the transition state than does the Ar migration in the case of R = OMe, and the tendency is the reverse for R = CO_2Et . These results mean that a favorable rearrangement reaction is the Ph migration for R = OMe and the Ar migration for R = CO_2Et , even if the initial structure is A or P. Therefore, it was clarified that the isomerization reaction of internal alkynes to vinylidenes proceeds through the direct 1,2-shift with the orientation changes of path 3, as shown in Scheme 6.

The NBO analysis of the TS structure provided essential information about whether the reaction is nucleophilic or electrophilic. In all cases, the minus charges of the carbon atoms within the appropriate migrating group are smaller than those of the carbon atoms in the stationary group. Although it seemed that the 1,2-aryl shifts are electrophilic reactions, donor–acceptor analysis dismisses this notion. The β -carbon in vinylidene accepts an electron from the migrating group under any circumstances. In addition, the 1,2-shift of the aryl group occurs more easily due to the large charge transfer from the aryl group to the CC triple bond. The migration reaction is not electrophilic but rather nucleophilic, and the migration aptitude depends on the charge transfer ability and the s character of the acceptor carbon. Moreover, the effect of substituent on the aromatic ring is important for the stabilization of positive charge on the acceptor carbon, and thus the migration of

electron-withdrawing or less electron-donating aryl group is preferable.

■ ASSOCIATED CONTENT

📄 Supporting Information

Contour plots of the donor and acceptor orbitals in Table 6, dihedral angles of the reactant and the product for paths 1–4 in Figure 1, and the absolute energies (in Hartrees) and the coordinates of the atoms in all the molecules whose geometries were optimized for stationary points. This material is available free of charge via the Internet at <http://pubs.acs.org>.

■ AUTHOR INFORMATION

Corresponding Author

tsuchida.noriko@ocha.ac.jp; takano.keiko@ocha.ac.jp

Present Address

[§]Department of Chemistry, Faculty of Science, Tokyo University of Science, 1–3 Kagurazaka, Shinjuku-ku, Tokyo 162–8601, Japan.

Notes

The authors declare no competing financial interest.

■ ACKNOWLEDGMENTS

We thank the Research Center for Computational Science in Okazaki, Japan, for the use of the computer facilities. This research was supported by a Grant-in-Aid for Scientific Research on Innovative Areas “Molecular Activation Directed toward Straightforward Synthesis” (23105543) from the MEXT of Japan.

■ REFERENCES

- (1) (a) Bruce, M. I. *Chem. Rev.* **1991**, *91*, 197–257. (b) Puerta, M. C.; Valerga, P. *1999*, 193–195, 977–1025.
- (2) (a) Schollhammer, P.; Cabon, N.; Capon, J. -F.; Petillon, F. Y.; Talarmin, J. *Organometallics* **2001**, *20*, 1230–1242. (b) Cabeza, J. A.; Perez-Carreño, E. *Organometallics* **2010**, *29*, 3973–3978.
- (3) (a) *Metal Vinylidenes and Allenylidenes in Catalysis: From Reactivity to Applications in Synthesis*; Bruneau, C., Dixneuf, P. H., Eds.; Wiley-VCH: Weinheim, Germany, 2008. (b) Bruneau, C.; Dixneuf, P. H. *Acc. Chem. Res.* **1999**, *32*, 311–323. (c) Katayama, H.; Ozawa, F. *Coord. Chem. Rev.* **2004**, *248*, 1703–1715. (d) Bruneau, C.; Dixneuf, P. H. *Angew. Chem.* **2006**, *45*, 2176–2203. (e) Varela, J. A.; Saá, C. *Chem.—Eur. J.* **2006**, *12*, 6450–6456. (f) Trost, B. M.; McClory, A. *Chem. Asian J.* **2008**, *3*, 164–194. (g) Trost, B. M.; Toste, F. D.; Pinkerton, A. B. *Chem. Rev.* **2001**, *101*, 2067–2096. (h) Alonso, F.; Beletskaya, I. P.; Yus, M. *Chem. Rev.* **2004**, *104*, 3079–3160. (i) Trost, B. M.; Frediksen, M. U.; Rudd, M. T. *Angew. Chem., Int. Ed.* **2005**, *44*, 6630–6666.
- (4) (a) Birdwhistell, K. R.; Tonker, T. L.; Templeton, J. L. *J. Am. Chem. Soc.* **1987**, *109*, 1401–1407. (b) Connelly, N. G.; Geiger, W. E.; Lagunas, M. C. *J. Am. Chem. Soc.* **1995**, *117*, 12202–12208. (c) Bustelo, E.; Carbó, J. J.; Lledós, A.; Mereiter, K. *J. Am. Chem. Soc.* **2003**, *125*, 3311–3321. (d) Cadierno, V.; Gamasa, M. P.; Gimeno, J.; Gonzalez-Bernardo, C. *Organometallics* **2001**, *20*, 5177–5188.

- (e) Swennenhuis, B. H. G.; Cieslinski, G. B.; Brothers, E. N.; Bengali, A. A. *J. Organomet. Chem.* **2010**, *695*, 891–897. (f) Wang, Q.; Wang, X.; Andrews, L. J. *Phys. Chem. A* **2011**, *115*, 12194–12200. (g) Lynam, J. M. *Chem.—Eur. J.* **2010**, *16*, 8238–8247.
- (5) (a) De Angelis, F.; Sgamellotti, A. *Organometallics* **2002**, *21*, 5944–5950. (b) De Angelis, F.; Sgamellotti, A. *Organometallics* **2002**, *21*, 2715–2723.
- (6) (a) Wakatsuki, Y.; Koga, N.; Yamazaki, H.; Morokuma, K. *J. Am. Chem. Soc.* **1994**, *116*, 8105–8111. (c) Tokunaga, M.; Suzuki, T.; Koga, N.; Fukushima, T.; Horiuchi, A.; Wakatsuki, Y. *J. Am. Chem. Soc.* **2001**, *123*, 11917–11924. (d) Wakatsuki, Y. *J. Organomet. Chem.* **2004**, *689*, 4092–4109.
- (7) (a) Pérez-Carreño, E.; Paoli, P.; Ienco, A.; Mealli, C. *Eur. J. Inorg. Chem.* **1999**, 1315–1324. (b) Vastine, B. A.; Hall, M. B. *Organometallics* **2008**, *27*, 4325–4333. (c) Wakatsuki, Y.; Koga, N.; Werner, H.; Morokuma, K. *J. Am. Chem. Soc.* **1997**, *119*, 360–366.
- (8) (a) Grotjahn, D. B.; Zeng, X.; Cooksy, A. L. *J. Am. Chem. Soc.* **2006**, *128*, 2798–2799. (b) Grotjahn, D. B.; Zeng, X.; Cooksy, A. L.; Kassel, W. S.; DiPasquale, A. G.; Zakharov, L. N.; Rheingold, A. L. *Organometallics* **2007**, *26*, 3385–3402. (c) De Angelis, F.; Sgamellotti, A.; Re, N. *Organometallics* **2007**, *26*, 5285–5288.
- (9) (a) Sakurai, H.; Hirama, K.; Nakadaira, Y.; Kabuto, C. *J. Am. Chem. Soc.* **1987**, *109*, 6880–6881. (b) Sakurai, H.; Fujii, T.; Sakamoto, K. *Chem. Lett.* **1992**, *21*, 339–342. (c) Connelly, N. G.; Geiger, W. E.; Lagunas, M. C.; Metz, B.; Rieger, A. L.; Rieger, P. H.; Shaw, M. J. *J. Am. Chem. Soc.* **1995**, *117*, 12202–12208. (d) Schneider, D.; Werner, H. *Angew. Chem. Int. Ed. Engl.* **1991**, *30*, 700–702. (e) Werner, H.; Baum, M.; Schneider, D.; Windmiüller, B. *Organometallics* **1994**, *13*, 1089–1097. (f) Windmiüller, H.; Onitsuka, K.; Ozawa, F. *Organometallics* **1996**, *15*, 4642–4645. (g) Werner, H.; Lass, R. W.; Gevert, O.; Wolf, J. *Organometallics* **1997**, *16*, 4077–4088. (h) Jiménez, M. V.; Sola, E.; Lahoz, F. J.; Oro, L. A. *Organometallics* **2005**, *24*, 2722–2729. (i) Ilg, K.; Paneque, M.; Poveda, M. L.; Rendon, N.; Santos, L. L.; Carmona, E.; Mereiter, K. *Organometallics* **2006**, *25*, 2230–2236. (j) Lass, R. W.; Werner, H. *Inorg. Chim. Acta* **2011**, *369*, 288–291. (k) Naka, A.; Okazaki, S.; Hayashi, M.; Ishikawa, M. *J. Organomet. Chem.* **1995**, *499*, 35–41. (l) Onitsuka, K.; Katayama, H.; Sonogashira, K.; Ozawa, F. *J. Chem. Soc., Chem. Commun.* **1995**, 2267–2268. (m) Katayama, H.; Ozawa, F. *Organometallics* **1998**, *17*, 5190–5196. (n) Huang, D.; Streib, W. E.; Eisenstein, O.; Caulton, K. G. *Organometallics* **2000**, *19*, 1967–1972. (o) Foerstner, J.; Kakoschke, A.; Goddard, R.; Rust, J.; Wartchow, R.; Butenschön, H. *J. Organomet. Chem.* **2001**, *617–618*, 412–422. (p) Foerstner, J.; Kakoschke, A.; Goddard, R.; Rust, J.; Wartchow, R.; Butenschön, H. *J. Organomet. Chem.* **2001**, *617–618*, 412–422. (q) Murakami, M.; Ubukata, M.; Ito, Y. *Chem. Lett.* **2002**, 294–295. (r) Murakami, M.; Hori, S. *J. Am. Chem. Soc.* **2003**, *125*, 4720–4721. (s) Miura, T.; Murata, H.; Kiyota, K.; Kusama, H.; Iwasawa, N. *J. Mol. Catal. A: Chem.* **2004**, *213*, 59–71. (t) Konkol, M.; Steinborn, D. *J. Organomet. Chem.* **2006**, *691*, 2839–2845.
- (10) Shaw, M. J.; Bryant, S. W.; Rath, N. *Eur. J. Inorg. Chem.* **2007**, 3943–3946.
- (11) (a) Ikeda, Y.; Yamaguchi, T.; Kanao, K.; Kimura, K.; Kamimura, S.; Mutoh, Y.; Tanabe, Y.; Ishii, Y. *J. Am. Chem. Soc.* **2008**, *130*, 16856–16857. (b) Mutoh, Y.; Ikeda, Y.; Kimura, Y.; Ishii, Y. *Chem. Lett.* **2009**, *38*, 534–535. (c) Mutoh, Y.; Imai, K.; Kimura, Y.; Ikeda, Y.; Ishii, Y. *Organometallics* **2011**, *30*, 204–207. (d) Mutoh, Y.; Kimura, Y.; Ikeda, Y.; Tsuchida, N.; Takano, K.; Ishii, Y. *Organometallics* **2012**, *31*, 5150–5158.
- (12) (a) de los Ríos, I.; Bustelo, E.; Puerta, M. C.; Valerga, P. *Organometallics* **2010**, *29*, 1740–1749. (b) Singh, V. K.; Bustelo, E.; de los Ríos, I.; Macias-Arce, I.; Puerta, M. C.; Valerga, P.; Ortuno, M. A.; Ujaque, G.; Lledos, A. *Organometallics* **2011**, *30*, 4014–4031.
- (13) Bassetti, M.; Cadierno, V.; Gimeno, J.; Pasquini, C. *Organometallics* **2008**, *27*, 5009–5016.
- (14) (a) Svensson, M.; Humbel, S.; Froese, R. D. J.; Matsubara, T.; Sieber, S.; Morokuma, K. *J. Phys. Chem.* **1996**, *100*, 19357–19363. (b) Dapprich, S.; Komaromi, I.; Byun, K. S.; Morokuma, K.; Frisch, M. J. *THEOCHEM* **1996**, *461*, 1–21.
- (15) (a) Becke, A. D. *J. Chem. Phys.* **1996**, *98*, 5648–5652. (b) Perdew, J. P.; Wang, Y. *Phys. Rev. B* **1992**, *45*, 13244–13249.
- (16) Rappe, A. K.; Casewit, C. J.; Colwell, K. S.; Goddard, W. A., III; Skiff, W. M. *J. Am. Chem. Soc.* **1992**, *114*, 10024–10035.
- (17) (a) Hay, P. J.; Wadt, W. R. *J. Chem. Phys.* **1985**, *82*, 270–283. (b) Hay, P. J.; Wadt, W. R. *J. Chem. Phys.* **1985**, *82*, 284–298. (c) Hay, P. J.; Wadt, W. R. *J. Chem. Phys.* **1985**, *82*, 299–310.
- (18) (a) Hehre, W. J.; Ditchfield, R.; Pople, J. A. *J. Chem. Phys.* **1972**, *56*, 2257–2261. (b) Francl, M. M.; Pietro, W. J.; Hehre, W. J.; Binkley, J. S.; Gordon, M. S.; DeFrees, D. J.; Pople, J. A. *J. Chem. Phys.* **1982**, *77*, 3654–3665.
- (19) Andrae, D.; Häußermann, U.; Dolg, M.; Stoll, H.; Preuß, H. *Theor. Chim. Acta* **1990**, *77*, 123–141.
- (20) Frisch, M. J.; Trucks, G. W.; Schlegel, H. B.; Scuseria, G. E.; Robb, M. A.; Cheeseman, J. R.; Scalmani, G.; Barone, V.; Mennucci, B.; Petersson, G. A.; Nakatsuji, H.; Caricato, M.; Li, X.; Hratchian, H. P.; Izmaylov, A. F.; Bloino, J.; Zheng, G.; Sonnenberg, J. L.; Hada, M.; Ehara, M.; Toyota, K.; Fukuda, R.; Hasegawa, J.; Ishida, M.; Nakajima, T.; Honda, Y.; Kitao, O.; Nakai, H.; Vreven, T.; Montgomery, Jr., J. A.; Peralta, J. E.; Ogliaro, F.; Bearpark, M.; Heyd, J. J.; Brothers, E.; Kudin, K. N.; Staroverov, V. N.; Kobayashi, R.; Normand, J.; Raghavachari, K.; Rendell, A.; Burant, J. C.; Iyengar, S. S.; Tomasi, J.; Cossi, M.; Rega, N.; Millam, J. M.; Klene, M.; Knox, J. E.; Cross, J. B.; Bakken, V.; Adamo, C.; Jaramillo, J.; Gomperts, R.; Stratmann, R. E.; Yazyev, O.; Austin, A. J.; Cammi, R.; Pomelli, C.; Ochterski, J. W.; Martin, R. L.; Morokuma, K.; Zakrzewski, V. G.; Voth, G. A.; Salvador, P.; Dannenberg, J. J.; Dapprich, S.; Daniels, A. D.; Farkas, O.; Foresman, J. B.; Ortiz, J. V.; Cioslowski, J.; Fox, D. J. *Gaussian 09, Revision A.02*; Gaussian, Inc.: Wallingford CT, 2009.
- (21) (a) Fukui, K. *J. Phys. Chem.* **1970**, *74*, 4161. (b) Gonzalez, C.; Schlegel, H. B. *J. Phys. Chem.* **1987**, *90*, 2154. (c) Gonzalez, C.; Schlegel, H. B. *J. Phys. Chem.* **1990**, *94*, 5523. (d) Gonzalez, C.; Schlegel, H. B. *J. Chem. Phys.* **1989**, *90*, 2154. (e) Fukui, K. *Acc. Chem. Res.* **1981**, *14*, 363. (f) Tomasi, J.; Persico, M. *Chem. Rev.* **1994**, *94*, 2027.
- (22) Reed, A. E.; Curtiss, L. A.; Weinhold, F. *Chem. Rev.* **1988**, *88*, 899–926.